



## Effect of Droplet Lifetime on Where Ions are Formed in Electro spray Ionization

Journal:	<i>Analyst</i>
Manuscript ID	AN-ART-09-2018-001824.R1
Article Type:	Paper
Date Submitted by the Author:	05-Nov-2018
Complete List of Authors:	Xia, Zijie; University of California, Berkeley Williams, Evan; University of California, Berkeley

1  
2  
3  
4  
5 Effect of Droplet Lifetime on Where Ions are Formed in Electrospray Ionization  
6  
7  
8  
9  
10  
11

12  
13 Zijie Xia<sup>1</sup> and Evan R. Williams<sup>1\*</sup>  
14  
15  
16  
17

18 *(1) Department of Chemistry, University of California, Berkeley, California 94720-1460*  
19  
20  
21  
22  
23  
24  
25  
26  
27  
28  
29  
30  
31  
32  
33  
34  
35  
36  
37  
38

39 Submitted to: *Analyst*  
40  
41

42 Date: September 20<sup>th</sup>, 2018  
43  
44  
45  
46  
47  
48  
49

50 \*Corresponding Author: Evan R. Williams  
51

52 Phone: (510) 643-7161  
53

54 e-mail: [erw@berkeley.edu](mailto:erw@berkeley.edu)  
55  
56  
57  
58  
59  
60

1  
2  
3  
4  
5  
6  
7  
8  
9  
10  
11  
12  
13  
14  
15  
16  
17  
18  
19  
20  
21  
22  
23  
24  
25  
26  
27  
28  
29  
30  
31  
32  
33  
34  
35  
36  
37  
38  
39  
40  
41  
42  
43  
44  
45  
46  
47  
48  
49  
50  
51  
52  
53  
54  
55  
56  
57  
58  
59  
60

**Abstract**

The location of gaseous ion formation in electrospray ionization under native mass spectrometry conditions was investigated using theta emitters with tip diameters between 317 nm and 4.4  $\mu\text{m}$  to produce droplets with lifetimes between 1 and 50  $\mu\text{s}$ . Mass spectra of  $\beta$ -lactoglobulin do not depend on instrument source temperatures between 160 and 300  $^{\circ}\text{C}$  with the smallest tips. A high charge-state distribution is observed for larger tips that produce droplets with lifetimes  $\geq 10 \mu\text{s}$  and this distribution increases at higher source temperatures. These and other results show that gaseous protein ions originating from the smallest droplets are formed outside of the mass spectrometer whereas the majority of protein ions formed from the larger droplets are formed inside of the mass spectrometer where thermal heating of the droplet and concomitant protein unfolding inside of the droplet occurs. These results show that small emitter tips are advantageous in native mass spectrometry by eliminating effects of thermal destabilization of proteins in droplets inside of the mass spectrometer, eliminating the effects of non-specific protein dimerization and aggregation that can occur in larger droplets that contain more than one protein molecule, and significantly reducing salt adduction.

## Introduction

Despite the widespread use of electrospray ionization (ESI) to produce gaseous ions from a diverse range of samples for analysis by mass spectrometry (MS), the mechanism by which these ions are produced is still debated.<sup>1-3</sup> In the ion evaporation mechanism, ions are ejected from small droplets owing to the high electric field at the droplet surface, and gaseous ions can be continuously produced throughout the droplet evaporation process.<sup>4,5</sup> In the charged residue mechanism, gaseous ions are formed upon solvent evaporation in the late stages of the droplet lifetime.<sup>6,7</sup> Other mechanisms based upon these principles have been proposed, such as the chain ejection model<sup>8</sup> and the charged residue-field emission model.<sup>9</sup> Extensive information about these mechanisms and evidence supporting various mechanisms has been reported elsewhere.<sup>5,7-9</sup>

Knowledge about *where* ions are formed is important for understanding the effects of instrument conditions on the appearance of mass spectra and for obtaining reliable reaction rates from reactions that occur in droplet mixing experiments. Information about the conformation of proteins or other biomolecules in solution is often inferred from the resulting charge-state distributions observed in ESI mass spectra, where higher charge states indicate more unfolded conformations than lower charge states, which are indicative of more folded structures.<sup>10-12</sup> Some instrument conditions can affect the observed charge-state distributions.<sup>13,14</sup> For example, high electrospray potentials can lead to the formation of high charge states in otherwise native mass spectrometry conditions. These high charge states are indicative of protein denaturation in the electrospray droplets due to droplet heating outside of the mass spectrometer as a result of the high electric field. This effect is the basis of the method called electrothermal supercharging and can be enhanced at elevated electrospray source temperatures illustrating that understanding the

1  
2  
3 effects of these two essential instrument parameters is critical for preserving information about  
4  
5 molecular conformation that exists in the original solution.<sup>14,15</sup>  
6

7  
8 Many studies indicate that desolvated ions are formed at or inside of the atmospheric-  
9  
10 interface of the mass spectrometer. Optical spectroscopic measurements by van Berkel and  
11  
12 coworkers showed that primarily dications of octaethylporphyrin exist in the ESI plume  
13  
14 whereas monocations were observed in the mass spectra indicating that the gaseous ions are  
15  
16 produced inside of the atmospheric interface.<sup>16</sup> In contrast, fluorescence measurements by  
17  
18 Zenobi and coworkers indicated that some gaseous rhodamine 6G ions are formed in the  
19  
20 plume.<sup>17</sup> Chait and coworkers found that higher metal capillary interface temperatures lead to  
21  
22 the formation of higher charge states of proteins in water/methanol solutions that contain  
23  
24 ammonium acetate but only for some proteins without ammonium acetate.<sup>13</sup> They  
25  
26 hypothesized that ammonium acetate affected the droplet lifetime and attributed the change in  
27  
28 the charge-state distribution with temperature to the droplets entering the interface prior to  
29  
30 gaseous ion formation.<sup>13</sup> A similar conclusion was reported from organic reactions that occur  
31  
32 in electrospray droplets.<sup>18</sup> Correlations between the time evolution of different intermediates  
33  
34 and the distance between the ESI emitter and instrument inlet suggest that there is a sudden  
35  
36 discontinuity in the droplet desolvation process that occurs in the MS inlet. Heating the transfer  
37  
38 tube between electrospray emitter and instrument inlet or increasing instrument inlet  
39  
40 temperature can also result in different reaction products and intermediates at the same distance,  
41  
42 which is consistent with the influence of instrument conditions on the MS results. In recent  
43  
44 droplet fusion experiments aimed at obtaining information about reaction rates, ion formation is  
45  
46 assumed to occur at the entrance of the mass spectrometer and this assumption is used to  
47  
48 establish a reaction time.<sup>19</sup>  
49  
50  
51  
52  
53  
54  
55  
56  
57  
58  
59  
60

1  
2  
3 A key advance to understanding where ion formation occurs is the ability to form  
4 droplets of different size and to measure their corresponding lifetimes. This can be done using  
5 theta-emitters in which two different solutions are mixed during the electrospray ionization  
6 process.<sup>20-24</sup> To obtain the droplet lifetimes, a unimolecular reaction with a known rate constant  
7 in solution is induced by mixing two solutions and the progress of the reaction is monitored  
8 using MS.<sup>22,23</sup> A unimolecular process is used because droplet evaporation rapidly increases  
9 reagent concentrations with time leading to a large increase in apparent bimolecular reaction  
10 rates in droplets although other factors may also play a role.<sup>18,25</sup> The folding of proteins initiated  
11 by mixing induced by the electrospray process has been used to establish droplet lifetimes.<sup>22,23</sup>  
12 An acidified solution containing a protein that is significantly denatured or unfolded is mixed  
13 with either pure water or an aqueous buffer solution to induce a pH jump upon mixing. The  
14 extent of folding that occurs inside of the electrospray droplet is inferred from the resulting  
15 charge-state distributions. The droplet lifetime depends on the solution flow rate, which can be  
16 changed by varying the emitter tip diameter or backing pressure applied to the solution. This  
17 method has been used to produce droplet lifetimes between 1 and ~20  $\mu\text{s}$  using theta emitters  
18 with tip diameters ranging from 246 nm to ~1.7  $\mu\text{m}$  and a backing pressure between 5 and 40  
19 psi.<sup>22-24</sup> A mixing time of 1  $\mu\text{s}$  is significantly shorter than that possible in conventional mixing  
20 apparatus and this mixing time can be achieved with a 1000 fold lower flow rate. This method  
21 has enabled investigations of fast peptide folding that occurs much too rapidly to be observed  
22 using other mixing methods.<sup>23,24</sup> The lifetime of droplets can be varied by changing the distance  
23 between the emitter tip and the mass spectrometer and by changing spray potentials.<sup>18,26</sup>  
24 Velocities of droplets have been measured optically to obtain information about how long the  
25 droplets spend outside of the mass spectrometer. In experiments in which mixing is induced  
26  
27  
28  
29  
30  
31  
32  
33  
34  
35  
36  
37  
38  
39  
40  
41  
42  
43  
44  
45  
46  
47  
48  
49  
50  
51  
52  
53  
54  
55  
56  
57  
58  
59  
60

1  
2  
3 upon droplet collisions, gaseous ion formation is assumed to occur at the entrance of the mass  
4 spectrometer in order to establish a droplet lifetime from these velocity measurements.<sup>19,26</sup>  
5  
6 Droplets formed from emitters with  $\sim 4 \mu\text{m}$  tip diameters with lifetimes ranging from 20 to 230  
7  
8  $\mu\text{s}$  were reported.<sup>26</sup>  
9  
10

11  
12 In this study, theta emitters with tip diameters ranging from 317 nm to 4.4  $\mu\text{m}$  are used to  
13 produce droplets with lifetimes between 1 and 50  $\mu\text{s}$ . The effects of instrument source  
14 temperature on  $\beta$ -lactoglobulin ions produced from buffered aqueous solutions using these  
15 varying droplet sizes were investigated. Results from these experiments clearly show that  
16 gaseous ions that originate from the smallest droplets are formed outside of the mass  
17 spectrometer whereas ions originating from the larger droplets are formed inside of the heated  
18 electrospray interface of the mass spectrometer. Moreover, these results demonstrate three  
19 significant advantages for using submicron tips in native mass spectrometry: the elimination of  
20 effects of source temperature on the resulting mass spectra, significant reduction of non-volatile  
21 salt adducts, and the elimination of non-specific dimerization or aggregation that can occur when  
22 multiple protein molecules are present in the initial droplet formed from larger emitters.  
23  
24  
25  
26  
27  
28  
29  
30  
31  
32  
33  
34  
35  
36  
37  
38  
39

## 40 **Experimental Method**

### 41 *Mass Spectrometry*

42  
43 Mass spectra are acquired using an LTQ mass spectrometer (Thermo Fisher Scientific,  
44 Waltham, MA, USA) with nanoelectrospray ionization (nano-ESI). Borosilicate theta  
45 capillaries (1.2 mm o.d./0.9 mm i.d., 0.15 mm septum thickness, Sutter Instruments, Novato,  
46 CA, USA) were pulled into emitters with tip outer diameters of  $317 \pm 14 \text{ nm}$  (shorter  
47 dimension 228 nm),  $1.7 \pm 0.1 \mu\text{m}$  (shorter dimension 1.1  $\mu\text{m}$ ), and  $4.4 \mu\text{m} \pm 0.1 \mu\text{m}$  (shorter  
48  
49  
50  
51  
52  
53  
54  
55  
56  
57  
58  
59  
60

1  
2  
3 dimension 2.1  $\mu\text{m}$ ) (Fig. 1). Borosilicate capillaries (1.0 mm o.d./0.78 mm i.d., Sutter  
4  
5 Instruments, Novato, CA, USA) are pulled into single barrel emitters with tip diameter of 1.7  
6  
7  $\mu\text{m}$ . Nano-ESI is initiated by applying a spray potential (+ 600 V – 1 kV) on 0.127 mm diameter  
8  
9 platinum wires that are inserted into the two barrels of the theta emitters or the single barrel  
10  
11 emitters and are in contact with the solutions containing proteins. The emitter tips are placed  
12  
13 approximately 1.5 to 2 mm away from the instrument entrance, and the spray voltage is kept as  
14  
15 low as possible while maintaining spray stability. A spray potential of 1.3 kV is used to induce  
16  
17 electrothermal supercharging.<sup>14</sup> A 10 psi backing pressure of nitrogen gas is applied on all the  
18  
19 theta emitters but not on the single barrel emitters. The instrument source temperature is adjusted  
20  
21 from 160  $^{\circ}\text{C}$  to 300  $^{\circ}\text{C}$ , keeping the other instrument parameters constant. The fraction of  
22  
23 unfolded protein in the ESI droplets immediately prior to ion formation is determined from the  
24  
25 ion abundances in the charge-state distributions using Equation 1,  
26  
27  
28  
29

$$30 \quad F = \frac{\sum_{un\text{folded}} I_i}{\sum_{total} I_i} \quad (1)$$

31  
32  
33  
34  
35 where  $I_i$  is the protein ion abundance for individual charge states corresponding to the highly  
36  
37 charged unfolded protein and the entire charge-state distribution. Ammonium acetate (AA),  
38  
39 ammonium bicarbonate (ABC), and lyophilized powder of  $\beta$ -lactoglobulin are from Sigma  
40  
41 Aldrich (St. Louis, MO) and were used without further purification.  
42  
43

#### 44 *Tryptophan Fluorescence*

45  
46  
47 Emission spectra resulting from tryptophan fluorescence of  $\beta$ -lactoglobulin in 100 mM  
48  
49 AA, 10 mM AA and 100 mM ABC are obtained with a FluoroMax-3 spectrometer (Horiba  
50  
51 Scientific, Kyoto, Japan). The sample is excited at 280 nm and the resulting emission is  
52  
53 measured from 200 nm to 390 nm. Both the entrance and exit slit widths are 2 nm. The inner  
54  
55 chamber temperature is raised from 25  $^{\circ}\text{C}$  to 87.5  $^{\circ}\text{C}$  ( $\pm 0.2$   $^{\circ}\text{C}$  tolerance) in 2.5  $^{\circ}\text{C}$  increments.  
56  
57  
58  
59  
60

1  
2  
3 The solution is equilibrated for five minutes at each temperature prior to measurements. Three  
4 emission scans are acquired, background subtracted, and averaged for each temperature. A  
5 gaussian fit is used to obtain the maximum of the emission peak of  $\beta$ -lactoglobulin tryptophan  
6 for the emission peak using OriginPro (Northampton, MA). Temperature melt curves are  
7 generated by plotting the maximum of the tryptophan emission peak as a function of  
8 temperature.  
9  
10  
11  
12  
13  
14  
15  
16  
17  
18

## 19 **Results and Discussion**

### 20 *Droplet Lifetimes*

21  
22 The lifetimes of droplets produced by nano-ESI using theta emitters depend on several  
23 factors, including the solution flow rate, which can be controlled by changing the diameter of the  
24 emitter tip or by varying the backing pressure, the spray voltage, and the distance between the  
25 emitter tip and the entrance of the mass spectrometer.<sup>22,23,26</sup> Droplets with lifetimes ranging from  
26  $\sim 1 \mu\text{s}$  to  $10 \mu\text{s}$  can be produced with tip sizes between 244 nm and  $\sim 1.5 \mu\text{m}$  using a backing  
27 pressure between 5 and 40 psi at a fixed distance of about 1 to 2 mm.<sup>22-24</sup> In order to extend the  
28 droplet lifetimes for this study, theta emitters with tip diameters of  $4.4 \mu\text{m} \pm 0.1 \mu\text{m}$  (shorter  
29 dimension  $2.1 \mu\text{m}$ ) were prepared and the droplet lifetime was determined as done previously  
30 using pH-induced folding of cytochrome *c* using a 10 psi backing pressure.<sup>23</sup> The lifetime of  
31 droplets produced by these larger emitters was measured by mixing an acidified solution  
32 containing cytochrome *c* with pure water to induce a pH jump upon droplet formation in the ESI  
33 process. Aqueous solutions of  $5 \mu\text{M}$  cytochrome *c* at two different pH values corresponding to  
34 the initial solution (1% acetic acid; pH = 2.8) and the final mixed solution (this solution mixed  
35 50/50 with pure water resulting in 0.5% acetic acid after mixing; pH = 3.0) were prepared and  
36  
37  
38  
39  
40  
41  
42  
43  
44  
45  
46  
47  
48  
49  
50  
51  
52  
53  
54  
55  
56  
57  
58  
59  
60

1  
2  
3 nano-ESI mass spectra were obtained (Fig. 2a and 2b, respectively). The charge-state  
4  
5 distributions of cytochrome *c* ions in both spectra are bimodal, with the summed intensity of  
6  
7 lower charge states (7+ to 10+) corresponding to  $2\% \pm 1\%$  and  $26\% \pm 1\%$  of the total protein ion  
8  
9 abundances in these respective solutions. Fast mixing of this initial cytochrome *c* solution with  
10  
11 pure water using the 4.4  $\mu\text{m}$  theta emitters induces protein folding in the nano-ESI droplets and  
12  
13 results in  $22\% \pm 1\%$  of total protein ion abundance in the 7+ to 10+ charge states (Fig. 2c). This  
14  
15 value is lower than the  $26\% \pm 1\%$  value measured under equilibrium conditions indicating that  
16  
17 the folding process is largely, but not entirely complete.  
18  
19

20  
21 The integrated rate equation for a two-state reaction (Eq. 2) is used to model cytochrome  
22  
23 *c* folding as a two-state process;  
24

$$25 \quad t = \tau \times \ln \frac{A_e - A_0}{A_e - A_t} \quad (2)$$

26  
27 where  $t$  is the reaction time,  $\tau$  is the folding time constant that depends on the protein and  
28  
29 solution composition,  $A_e$ ,  $A_0$ , and  $A_t$  are the abundances of the folded protein at equilibrium, time  
30  
31 0 and time  $t$ , respectively. The folding time constant depends on many factors including the ionic  
32  
33 strength and composition of the solution. Droplet evaporation can also lead to pH changes in  
34  
35 unbuffered solutions that can affect protein folding rates.<sup>27</sup> All these factors result in some  
36  
37 uncertainty in the droplet lifetime obtained from these measurements for the large tip size.  
38  
39 Cytochrome *c* has a folding time constant of 57  $\mu\text{s}$  in 50 mM sodium acetate and 50 mM sodium  
40  
41 phosphate.<sup>28</sup> Previous results obtained from ammonium acetate solution at the same ionic  
42  
43 strength and in pure water indicate that the folding time constant  $\tau$  in pure water is about half  
44  
45 that in ammonium acetate (Table S-1). Thus, the droplet lifetime for the 4.4  $\mu\text{m}$  theta emitters  
46  
47 with a 10 psi backing pressure in these experiments obtained from the Figure 2 is  $\sim 50 \pm 7 \mu\text{s}$ .  
48  
49  
50  
51  
52  
53  
54  
55  
56  
57  
58  
59  
60

1  
2  
3 Droplet lifetimes in ESI have also been estimated from micro-particle image velocimetry  
4 measurements, which showed that 4  $\mu\text{m}$  theta emitters produced droplets with lifetimes between  
5  
6 20  $\mu\text{s}$  and 320  $\mu\text{s}$  depending on the spray voltage and the distance between emitter tip and the  
7  
8 instrument entrance (between 0.5 mm and 3 mm).<sup>26</sup> In the experiments here, the theta emitters  
9  
10 are about 1.5 mm to 2 mm away from the instrument entrance and the droplets are formed with  
11  
12 ~1 kV applied to the solution. Jansson et al. reported 73  $\mu\text{s}$  to 133  $\mu\text{s}$  for the similar spray voltage  
13  
14 and tip position.<sup>26</sup> Despite the significant differences in experimental methodologies, the droplet  
15  
16 lifetime measured with both techniques are remarkably similar.  
17  
18  
19  
20  
21  
22  
23

#### 24 *Effects of Droplet Lifetime and Source Temperature on Protein Unfolding in Droplets*

25

26 In order to answer the question about where desolvated gaseous protein ions are  
27  
28 formed during electrospray ionization, theta emitters with diameters of 317 nm, 1.7  $\mu\text{m}$  and  
29  
30 4.4  $\mu\text{m}$  were used to produce droplets with lifetimes ranging from 1  $\mu\text{s}$  to 50  $\mu\text{s}$ .<sup>23,29</sup> Even  
31  
32 though both channels of the theta emitters contain the same solution, theta emitters are used in  
33  
34 these experiments because the lifetimes of the droplets have been established with these  
35  
36 emitters<sup>22,23,29</sup> and knowledge of droplet lifetimes are important in understanding where  
37  
38 desolvated ions are formed. The instrument source temperature was varied between 160 °C and  
39  
40 300 °C to investigate effects, if any, of thermal activation of droplets that may enter the mass  
41  
42 spectrometer inlet system. The spray voltage was kept as low as possible while still maintaining  
43  
44 a stable spray to avoid electrothermal supercharging.<sup>14,15</sup> Experiments were performed with  $\beta$ -  
45  
46 lactoglobulin, which is a major whey protein in cow and goat milk because the thermal stability  
47  
48 of this protein has been widely studied under different pH and salt conditions.<sup>30-33</sup> The melting  
49  
50 temperature of  $\beta$ -lactoglobulin is reported in various studies to be between 70 and 80 °C at  
51  
52  
53  
54  
55  
56  
57  
58  
59  
60

1  
2  
3 neutral pH.<sup>31,33</sup>  $\beta$ -lactoglobulin has pI at 5.1 and is negatively charged in the aqueous buffered  
4 solutions used in these experiments.<sup>30</sup> Thus, these protein ions in solution should not interact  
5 significantly with the glass surface of the theta emitters, which can also induce protein  
6 destabilization and partial unfolding in solution before electrospray droplet formation.<sup>34,35</sup>  
7  
8  
9  
10  
11

12 Results for  $\beta$ -lactoglobulin (10  $\mu$ M in 100 mM ABC) obtained with 317 nm theta emitters  
13 at source temperatures between 160 °C and 300 °C are shown in Figure 3a-c. Charge states  
14 between 7+ and 9+ are observed, and the relative abundances of these charge states do not  
15 change significantly with instrument source temperature. In striking contrast, nano-ESI spectra  
16 obtained from this same solution using 4.4  $\mu$ m theta emitters show a charge-state distribution  
17 that is shifted to slightly higher charge at 160 °C (Fig. 3d) and the appearance of a second higher  
18 charge-state distribution (11+ to 17+) centered at 14+ that increases in relative abundance with  
19 increasing source temperature (Fig. 3e and 3f). The higher charge-state distribution is indicative  
20 of a small population of unfolding proteins *in solution* that increases with source temperature.  
21  
22 The fraction of  $\beta$ -lactoglobulin that is unfolded in solution was estimated from the abundances of  
23 the 11+ to 17+ ions divided by the total protein ion signal (Eq. 1). These values obtained from  
24 the 4.4  $\mu$ m emitters are 1.7%  $\pm$  1.1%, 7.6%  $\pm$  3.4%, and 18.1%  $\pm$  1.3% at source temperatures  
25 of 160 °C, 230 °C and 300 °C, respectively. It should also be noted that the charge-state  
26 distribution of the folded form of the protein is shifted from 8+ with the 317 nm emitters to 9+  
27 with the 4.4  $\mu$ m suggesting that the native structure of the protein may be partially destabilized  
28 with the larger emitter at all source temperatures, although other factors may also contribute.  
29  
30 Heating the instrument source increases the surrounding air temperature, and some heating of the  
31 solution in the emitter tip and the droplets may also occur before the droplets enter the mass  
32 spectrometer. The air temperature measured near the instrument source increases slightly from  
33  
34  
35  
36  
37  
38  
39  
40  
41  
42  
43  
44  
45  
46  
47  
48  
49  
50  
51  
52  
53  
54  
55  
56  
57  
58  
59  
60

1  
2  
3 38 °C to 48 °C when the instrument source temperature increases from 160 °C to 300 °C. This  
4  
5 does not appear to impact the structure of the protein in the emitter tip because no change in the  
6  
7 charge-state distribution is observed with the smallest theta emitters and this range of  
8  
9 temperatures is below the melting transition of this protein. A similar trend in increasing  
10  
11 unfolded population with increasing source temperature occurs with 1.7 μm theta emitters (Fig.  
12  
13 S-1 a-c) but to a lesser extent than with the 4.4 μm theta emitters. In striking contrast, the  
14  
15 fraction of ions corresponding to an unfolded protein formed from 317 nm theta emitters is less  
16  
17 than 1%, and there is no trend with increasing source temperature. The trend of increasing  
18  
19 unfolded protein population with increasing instrument source temperature indicates that the  
20  
21 droplets generated from 1.7 μm and 4.4 μm theta emitters experience the high temperature inside  
22  
23 the heated ion transfer tube of the instrument. As the larger droplets are heated inside the ion  
24  
25 transfer tube of the instrument source, some protein melting or unfolding occurs inside the  
26  
27 droplets. The population of unfolded molecules in the droplets will lead to higher charge states  
28  
29 whereas those that are still folded will lead to the lower charge states. Once bare ions are  
30  
31 formed, conformational changes may occur as a result of heating, but these conformational  
32  
33 changes will not lead to changes in the ion charge states. Therefore, these charge state changes  
34  
35 that are observed from 1.7 μm and 4.4 μm theta emitters are a result of conformational changes  
36  
37 that occur in the droplets. Protein ion peaks are also broader from 1.7 μm and 4.4 μm emitters  
38  
39 than the ones formed from 317 nm emitters due to sodium adducts, which is consistent with  
40  
41 previously reported desalting effects of submicron single and theta emitters during electrospray  
42  
43 ionization.<sup>34,36–38</sup>  
44  
45  
46  
47  
48  
49  
50

51 The temperature inside of the ion transfer tube is likely to be much lower than the  
52  
53 elevated set temperature owing to the heat transfer between room temperature air and the heated  
54  
55  
56  
57  
58  
59  
60

1  
2  
3 ion transfer tube. The droplet temperature can be further reduced as a result of evaporative  
4 cooling. Thus, the temperatures of the larger droplets inside the transfer tube is unknown. To  
5 confirm that the low charge state ions produced from the larger droplets at higher temperature  
6 are formed inside the source and not before entering the mass spectrometer, the native form of  $\beta$ -  
7 lactoglobulin was destabilized by adding 3% (v/v) ammonium hydroxide in 100 mM ABC (pH  
8 10). A nano-ESI spectrum obtained with the 317 nm theta emitters at a source temperature of  
9 160 °C shows that approximately 5% of the protein is unfolded in this solution (Fig. S-2),  
10 consistent with the native form of the protein somewhat destabilized so that both folded and  
11 unfolded forms are in equilibrium. Even with a 300 °C source temperature, there is no significant  
12 increase of unfolded protein with the small emitters (Fig S-2 a-b), consistent with the hypothesis  
13 that the droplets generated from the submicron theta emitters do not experience the high  
14 temperature inside the source. In striking contrast, 66% of the ion population formed using the  
15 4.4  $\mu\text{m}$  theta emitters corresponds to proteins that are unfolded in solution at a source  
16 temperature of 300 °C (Fig S-2 c-d). This indicates that the majority of the droplets formed by  
17 the larger emitters enter the source and that heat from the source results in melting of the protein  
18 in solution inside of the mass spectrometer prior to protein ion formation. It appears from these  
19 results that the droplets are insufficiently heated even at this source temperature to completely  
20 unfold the protein in solution under these conditions, consistent with results from a prior study.<sup>13</sup>  
21  
22  
23  
24  
25  
26  
27  
28  
29  
30  
31  
32  
33  
34  
35  
36  
37  
38  
39  
40  
41  
42  
43  
44  
45

#### 46 *Droplet Velocities and Location of Ion Formation*

47  
48  
49 In order to more thoroughly understand why the charge-state distribution of ions formed  
50 from the smallest theta emitters are not affected by the temperature of the source whereas the  
51 droplets formed from the larger emitters are affected, the initial droplet velocities and air flow  
52  
53  
54  
55  
56  
57  
58  
59  
60

1  
2  
3 velocity through the heated ion transfer tube were determined. The initial droplet velocity with  
4 the 317 nm theta emitters is about 2 m/s.<sup>1</sup> The initial velocity of droplets formed from larger  
5 emitters is even less (estimated to be about 0.25 m/s with the 4.4 μm theta emitters based on a  
6 flow rate of 3461 ± 509 pL/s). The theta emitters are approximately 1.5 mm to 2 mm away from  
7 the instrument entrance, so this initial velocity is insufficient for the smallest nanodrops that have  
8 a 1 μs lifetime to reach the mass spectrometer. However, the droplets are accelerated by the  
9 applied electric field, and this force is resisted by collisions with the ambient background gas.  
10 There is also gas flow into the mass spectrometer induced by the pressure difference between  
11 where the ions are formed (~760 Torr) and the first vacuum stage (~0.6 Torr). The air flow into  
12 the instrument was estimated using a simplified Hagen-Poiseuille equation for viscous airflow  
13 (Eq. 3).

$$C = \frac{\pi d^4}{128\mu l} * \frac{(P_1 + P_2)}{2} \quad (3)$$

14  
15  
16  
17  
18  
19  
20  
21  
22  
23  
24  
25  
26  
27  
28  
29  
30  
31  
32 Where  $d$  is the diameter of instrument entrance (0.58 mm),  $l$  is the length of the ion transfer tube  
33 (58.42 mm),  $\mu$  is the viscosity of air in Poise,  $P_1$  and  $P_2$  are the pressures before and after the ion  
34 transfer tube. The viscosity of air changes from 1.82x10<sup>-4</sup> Poise to 2.98x10<sup>-4</sup> Poise with  
35 increasing temperature from 20 °C to 300 °C. This is a relatively small change, and the  
36 temperature of the air is significantly lower than the set temperature of 300 °C of the ion transfer  
37 tube. Thus, the viscosity of air at room temperature was used to obtain an estimate of the air  
38 flow conductance into the instrument. The calculated air flow conductance is 0.102 L/s, and the  
39 air flow velocity inside of the transfer tube is 386 m/s. The airflow velocity between the emitter  
40 and the source should be less, but the electrostatic force should result in a higher velocity of the  
41  
42  
43  
44  
45  
46  
47  
48  
49  
50  
51  
52  
53  
54

---

55  
56 <sup>1</sup> The previously reported values from Mortensen et al. were mislabeled as m/s instead of the correct unit of mm/s.  
57  
58  
59  
60

1  
2  
3 droplet than that of the air itself. If the droplet velocity outside the mass spectrometer is roughly  
4  
5 the same as the air flow velocity through the ion transfer tube, then the droplets formed from  
6  
7 theta emitters would have to last at least 5  $\mu\text{s}$  in order to enter the instrument entrance as intact  
8  
9 droplets. The 1  $\mu\text{s}$  lifetime of droplets formed by the 317 nm theta emitters is much too short  
10  
11 indicating that the desolvated gaseous ions must be formed outside of the mass spectrometer.  
12  
13 This result is consistent with the observation that the charge-state distribution obtained with  
14  
15 these small emitters do not depend on the source temperature. In contrast, the 1.7  $\mu\text{m}$  and 4.4  
16  
17  $\mu\text{m}$  theta emitters generate droplets that survive for about 10  $\mu\text{s}$  and 50  $\mu\text{s}$ , respectively. These  
18  
19 lifetimes are sufficient that the majority of the droplets enter the ESI interface of the mass  
20  
21 spectrometer before gaseous ion formation occurs, consistent with the protein melting observed  
22  
23 inside the droplets at the higher source temperatures.  
24  
25  
26  
27

28         Significantly lower droplet velocities between 8 and 23 m/s were reported by Jansson et al.  
29  
30 with 4  $\mu\text{m}$  diameter emitters over a range of distance and spray voltages.<sup>26</sup> The flow of air  
31  
32 through the ion transfer tube should be similar in those experiments. If the droplet velocities in  
33  
34 our experiments are at the highest velocity of 23 m/s reported by Jansson et al., then it would  
35  
36 require  $\sim 65$   $\mu\text{s}$  for these droplets to reach the source. However, our results indicate that the  
37  
38 droplets formed from 1.7  $\mu\text{m}$  emitters which have a lifetime of 10  $\mu\text{s}$  do in fact experience the  
39  
40 higher temperature inside the ion transfer tube. Thus, we conclude that the droplets on our  
41  
42 experiments must be moving at a higher velocity. This discrepancy between the droplet  
43  
44 velocities reported by Jansson et al. and the results of our experiments may be related to  
45  
46 assumptions made in the earlier experiments. Jansson et al. reported that the droplets formed  
47  
48 from 4  $\mu\text{m}$  theta emitters are around 4.3  $\mu\text{m}$  in diameter.<sup>26</sup> However, results from other studies  
49  
50 using similar emitters indicate that the initial size of the majority of droplets that result in  
51  
52  
53  
54  
55  
56  
57  
58  
59  
60

1  
2  
3 charged analyte ions is about 1/10 to 1/17 of the electrospray emitter diameter.<sup>36,39,40</sup> For  
4  
5 example, Bush and coworkers reported that the initial droplets formed from single barrel emitters  
6  
7 with diameters of ~1 to 3  $\mu\text{m}$  using common native electrospray conditions are approximately 60  
8  
9 nm in diameter.<sup>40</sup> Jansson et al. measured the droplet sizes optically using a setup where a single  
10  
11 pixel in their CCD camera corresponds to ~0.8  $\mu\text{m}$ .<sup>26</sup> Thus, this optical detection method is not  
12  
13 capable of measuring the < 0.4  $\mu\text{m}$  droplets that result in protein ions observed in the mass  
14  
15 spectrometer. Although larger droplets may be formed as well, these droplets may not produce  
16  
17 the majority of the protein ions that are observed. It should also be emphasized that reaction  
18  
19 kinetics that have been reported previously based on optically measured velocities have included  
20  
21 the explicit assumption that bare protein ion formation occurs at the entrance of the mass  
22  
23 spectrometer.<sup>26</sup> Our results reported here clearly show that this is not the case. The similar  
24  
25 droplet lifetimes for the 4  $\mu\text{m}$  emitters deduced from these two experiments may be a result of an  
26  
27 underestimation of both the droplet velocity and the distance traveled prior to ion formation in  
28  
29 the optical-based studies.  
30  
31  
32  
33  
34  
35  
36  
37

### 38 *Buffer Effect on Protein Unfolding in Droplets*

39

40 It is well known that different buffers can stabilize or destabilize the native forms of  
41  
42 proteins. Ammonium acetate is a more commonly used buffer in native mass spectrometry  
43  
44 experiments than ammonium bicarbonate despite the fact that ammonium acetate is a poor  
45  
46 buffer at neutral pH.<sup>41</sup> The effect of ammonium acetate on the extent of thermal induced  
47  
48 protein unfolding in longer-lived droplets was investigated by measuring nano-ESI mass  
49  
50 spectra of  $\beta$ -lactoglobulin (10  $\mu\text{M}$ ) in 100 mM AA using 317 nm, 1.7  $\mu\text{m}$ , and 4.4  $\mu\text{m}$  theta  
51  
52  
53  
54  
55  
56  
57  
58  
59  
60

1  
2  
3 emitters at instrument source temperatures between 160 °C and 300 °C (Fig. 4 and Fig. S-1 d-f).  
4  
5 With 317 nm emitters, the spectra are similar to those formed under the same conditions but with  
6  
7 100 mM ABC and there is no dependence on source temperature. Results with the 4.4 μm theta  
8  
9 emitters show there is a source temperature dependence, as was the case with 100 mM ABC, but  
10  
11 the fraction of unfolded protein is much less at higher temperatures. At 230 °C, the fraction of  
12  
13 unfolded β-lactoglobulin is  $3.4\% \pm 1.5\%$ , which is approximately half that from 100 mM ABC.  
14  
15 At 300 °C, the fraction of the unfolded protein is  $7.2\% \pm 1.5\%$ , again, less than half that from  
16  
17 100 mM ABC (Fig. 4). A similar trend of the formation of unfolded protein from 100 mM AA is  
18  
19 observed using 1.7 μm theta emitters (Fig. S-1 d-f). The increasing trend of the unfolded protein  
20  
21 with increasing source temperature from 100 mM AA using larger theta emitters is consistent  
22  
23 with the hypothesis that protein ions formed from larger theta emitters are formed inside the  
24  
25 heated ion transfer tube, which causes thermal denaturation of the protein. However, it appears  
26  
27 that less unfolding occurs with 100 mM AA than with 100 mM ABC. This is also consistent  
28  
29 with the 8+ being the most abundant ion with AA, but the 9+ is most abundant with ABC at this  
30  
31 same emitter size. It is also interesting to note that dimer abundance is significantly higher in the  
32  
33 spectra obtained from the AA solution.  
34  
35  
36  
37  
38  
39

40 Ionic strength can affect protein conformation and stability.<sup>42</sup> These experiments were  
41  
42 repeated in 10 mM AA (Fig S-3). There is no significant change in the charge-state distribution  
43  
44 with source temperature using 317 nm theta emitters, but there is an increase in the abundance of  
45  
46 unfolded protein with 4.4 μm emitters with increasing temperature. The fraction of unfolded  
47  
48 protein formed from the 10 mM AA solution is slightly higher than that formed from the 100  
49  
50 mM AA solution at high source temperature with both the 1.7 μm and 4.4 μm emitters (Fig. 5).  
51  
52  
53  
54  
55  
56  
57  
58  
59  
60

1  
2  
3 This result is consistent with lower ionic strength causing a small reduction in the stability of the  
4 folded form of the protein.  
5  
6

7  
8 The effects of these buffers on the stability of the native form of  $\beta$ -lactoglobulin were  
9 studied with fluorescence. Upon thermal denaturation, exposure of tryptophan to solvent  
10 typically increases the fluorescent emission intensity. However, for  $\beta$ -lactoglobulin, tryptophan  
11 fluorescence emission intensity decreases with increasing temperature (Fig. S-4). This  
12 phenomenon has been attributed to the thermal deactivation of the tryptophan fluorophores or the  
13 change in tertiary structure resulting in increasing proximity between primary amines of lysine  
14 residues and tryptophan fluorophores, which leads to fluorescent quenching.<sup>31,43</sup> A measure of  
15  $\beta$ -lactoglobulin unfolding can also be obtained from the wavelength of the maximum of the  
16 tryptophan emission peak, which provides a measure of the polarity of the environment around  
17 tryptophan. As  $\beta$ -lactoglobulin unfolds, tryptophan that is buried inside the fully folded protein  
18 in a less polar environment transitions to exposure to polar solvent in the unfolded state.<sup>31</sup>  
19  
20  
21  
22  
23  
24  
25  
26  
27  
28  
29  
30  
31  
32

33 Temperature melting curves for  $\beta$ -lactoglobulin in the three different buffers were obtained by  
34 plotting the wavelength of the tryptophan emission peak maximum as a function of temperature  
35 (Fig. 6). The melting curves obtained from 10 mM AA and 100 mM AA are similar, but between  
36 50 °C and 70 °C, the wavelength maximum is consistently higher from 10 mM AA compared to  
37 that from 100 mM AA, indicating more exposure of tryptophan to the polar solvent at lower AA  
38 concentration within this temperature range. In contrast, the melting curve obtained from 100  
39 mM ABC shows that considerably more unfolding occurs at a lower temperature compared to  
40 either AA solution. These results show that  $\beta$ -lactoglobulin is thermally less stable in ABC than  
41 AA even at the same ionic strength. The fluorescence results from the three different buffers  
42 support the observation that more thermal unfolding occurs in droplets that are heated by the  
43  
44  
45  
46  
47  
48  
49  
50  
51  
52  
53  
54  
55  
56  
57  
58  
59  
60

1  
2  
3 source for ABC than it does for AA. It is interesting that the air near the instrument source can  
4 reach 50 °C, a temperature at which some unfolding should occur in ABC, yet no significant  
5 unfolding is observed with the 317 nm theta emitters. Either the nanodrops have lifetimes that  
6 are too short to experience these elevated temperatures as droplets or evaporative cooling of the  
7 droplet may compete with resistive and ambient heating resulting in a somewhat lower  
8 temperature in the droplet compared to the ambient air.  
9  
10  
11  
12  
13  
14  
15  
16  
17  
18

### 19 *Droplet Size Effect on Protein Dimerization*

20  
21 It is interesting to note that there is substantial dimer signal in the mass spectra obtained  
22 with the 1.7  $\mu\text{m}$  and 4.4  $\mu\text{m}$  theta emitters but not with the 317 nm emitters with the 100 mM AA  
23 solution (Fig. 4).  $\beta$ -lactoglobulin is predominantly a dimer at physiological conditions ( $> 50 \mu\text{M}$   
24 protein concentration), and the dimer-monomer equilibrium depends on pH, buffer, and ionic  
25 strength.<sup>44</sup> Because the protein concentration in these studies is low, there should be a relatively  
26 low concentration of protein dimers in solution. With the 317 nm theta emitters, less than 9% of  
27 the total protein ion signal corresponds to the  $\beta$ -lactoglobulin dimer. However, the dimer  
28 abundance is up to 35% with the 1.7  $\mu\text{m}$  and 4.4  $\mu\text{m}$  emitters (Fig. 4 and Fig S-1 d-f). We  
29 hypothesize that the dimer abundance is related to the presence of multiple protein molecules in  
30 large droplets produced by the larger emitters. If the initial droplet diameter is  $\sim 1/17$  the  
31 diameter of the theta emitter,<sup>40</sup> the initial droplet size for the 317 nm theta emitters is about 18  
32 nm (approximating the theta emitter as a single barrel emitter). At this initial droplet size, only 1  
33 out of  $\sim 60$  nanodrops that are formed contains a protein molecule. Unless the protein molecule  
34 enters the droplet in the dimeric form, it is an extremely low probability event for a droplet to  
35  
36  
37  
38  
39  
40  
41  
42  
43  
44  
45  
46  
47  
48  
49  
50  
51  
52  
53  
54  
55  
56  
57  
58  
59  
60

1  
2  
3 contain two individual protein molecules. Thus, the protein dimer ions from 317 nm theta  
4 emitters likely exist as molecular dimers in the bulk solution.  
5  
6

7  
8 The initial droplet diameters of a 1.7  $\mu\text{m}$  and 4.4  $\mu\text{m}$  theta emitter are 100 nm and 261  
9 nm, respectively. A 100 nm nanodrop contains on average slightly fewer than three protein  
10 molecules per droplet whereas a 261 nm droplet initially contains about 50 protein molecules.  
11  
12 Because the initial droplets may contain more than two protein molecules, the formation of  $\beta$ -  
13 lactoglobulin dimer can occur within the droplets as solvent evaporation occurs and the  
14 concentration of protein in the shrinking droplets increases. Thus, the extent of dimer ions  
15 observed in the nano-ESI mass spectra obtained with 317 nm emitters more accurately reflects  
16 the dimer concentrations in the original solution compared to the results from larger emitter sizes  
17 when dimers are formed as droplets evaporate during the ESI process.  
18  
19  
20  
21  
22  
23  
24  
25  
26  
27

28 The abundance of the protein dimers decreases with increasing instrument source  
29 temperature. For mass spectra obtained using 4.4  $\mu\text{m}$  theta emitters, the fraction of protein dimer  
30 out of total protein ion signals is  $30\% \pm 1\%$ ,  $24\% \pm 3\%$ , and  $19\% \pm 1\%$  at source temperatures  
31 of 160  $^{\circ}\text{C}$ , 230  $^{\circ}\text{C}$ , and 300  $^{\circ}\text{C}$ , respectively. The decrease in protein dimer abundance with  
32 increasing temperature indicates that the protein dimer thermally dissociates into monomers in  
33 the droplets. Although dimeric protein ions are also observed in mass spectra obtained for  $\beta$ -  
34 lactoglobulin in 10 mM AA and 100 mM ABC using 1.7  $\mu\text{m}$  and 4.4  $\mu\text{m}$  theta emitters, the  
35 abundance of protein dimer is much lower than in 100 mM AA (Fig. 3, Fig. S-1 a-c, Fig. S-3 d-  
36 i). Higher ionic strength favors dimer formation.<sup>44</sup> The absence of dimer ions with ABC may  
37 indicate that the native structures are sufficiently destabilized that the equilibrium disfavors the  
38 formation of the dimer in this buffer.  
39  
40  
41  
42  
43  
44  
45  
46  
47  
48  
49  
50  
51  
52  
53  
54  
55  
56  
57  
58  
59  
60

### *Electrothermal Supercharging Mechanism*

Results from these temperature melt studies provide additional insights into the mechanism of electrothermal supercharging.<sup>14,15</sup> Prior results indicate that proteins which have native forms in bulk solution can be rapidly denatured prior to their entrance into the mass spectrometer within the droplets due to a rise in droplet temperature as a result of resistive heating of the droplet induced by higher electrospray voltages.<sup>14</sup> The fluorescence results (Fig. 6) provide insights into why the effectiveness of this method depends on buffer identity.

To determine how emitter size, source temperature, and buffer identity affects electrothermal supercharging, mass spectra of  $\beta$ -lactoglobulin (10  $\mu$ M) from 100 mM ABC and 100 mM AA solutions were obtained using 1.7  $\mu$ m single barrel emitters at three instrument source temperatures at 1.3 kV and 800 V, respectively (Fig. 7 and Fig. S-5). Single barrel emitters were used in order to more directly compare with previous protein electrothermal supercharging results. As reported previously, very little supercharging occurs in AA regardless of source temperatures (Fig. 7a-c).<sup>15</sup> There is a slight increase in the average charge state with increasing source temperature as was observed at lower spray voltages. It is interesting to note that the extent of thermal denaturation of the protein at high source temperature even at 1.3 kV with single barrel emitters is lower than it is with low spray voltage using similar size theta emitters. The difference is likely due to the absence of backing pressure for single barrel emitter, which should result in a shorter droplet lifetime for similar size emitters. Mortensen et al. previously showed that decreasing backing pressure from 10 psi to 5 psi decreases the droplet lifetime by half.<sup>23</sup>

Electrothermal supercharging does occur for  $\beta$ -lactoglobulin in ABC at 1.3 kV, and the fraction of unfolded protein increases with increasing source temperature (Fig. 7 d-f). These

1  
2  
3 results from the two buffers are consistent with those of previous studies.<sup>14,15</sup> The abundances of  
4 the 10+ and 11+ charge states formed at 1.3 kV increase with increasing temperature and appear  
5 to correspond to unfolding intermediates. Similar results are obtained with theta emitters at  
6  
7 300 °C and at 1.3 kV spray voltage (Fig. S-6) indicating that this is not unique to single barrel  
8 emitters. The difference observed between purely source temperature induced heating and  
9 electrothermal supercharging indicates that the mechanism for electrothermal supercharging may  
10 be more complex and involve the kinetics of folding and unfolding. The higher electric field in  
11 electrothermal supercharging heats up the droplets *outside* of the mass spectrometer. Upon  
12 entering the ion transfer tube, evaporative cooling would lead to a steady state temperature that  
13 would occur in the absence of electrothermal supercharging. This rapid heating and subsequent  
14 cooling could trap unfolding intermediates that may not otherwise be observed in conventional  
15 heating experiments. Recent ion mobility results exploring unfolding of ubiquitin upon laser  
16 heating different size droplets has provided evidence for short-lived unfolding intermediates.<sup>45</sup>  
17  
18  
19  
20  
21  
22  
23  
24  
25  
26  
27  
28  
29  
30  
31  
32  
33  
34

## 35 Conclusions

36  
37  
38 The lifetime of droplets formed by nano-ESI can be varied between 1 and 50  $\mu\text{s}$  by  
39 changing the diameter of theta emitter tips from 317 nm to 4.4  $\mu\text{m}$ . The location of where ions  
40 are formed during nano-ESI from buffered aqueous solutions, whether inside or outside of the  
41 mass spectrometer, can be determined from the extent to which high charge-state distributions  
42 are induced by increasing the electrospray interface temperature. With 317 nm tips, which  
43 produce droplets that last about 1  $\mu\text{s}$ , only low charge state ions of  $\beta$ -lactoglobulin are observed  
44 at all instrument source temperatures for solutions consisting of ammonium acetate or  
45 ammonium bicarbonate. Very few high charge states are observed under basic conditions in  
46  
47  
48  
49  
50  
51  
52  
53  
54  
55  
56  
57  
58  
59  
60

1  
2  
3 which the native form of the protein is destabilized. In contrast, a higher charge-state  
4  
5 distribution, indicative of unfolded protein molecules in solution, is observed with 1.7 and 4.4  
6  
7  $\mu\text{m}$  theta emitters and this population increases with temperature. These results indicate that  
8  
9 droplets with lifetimes of  $\sim 1 \mu\text{s}$  do not survive long enough to enter the source inlet capillary and  
10  
11 that ions are formed outside of the mass spectrometer. In contrast, droplets formed from micron  
12  
13 size emitters with lifetimes  $\geq 10 \mu\text{s}$  enter the mass spectrometer and are heated inside of the  
14  
15 transfer tube prior to ion formation. This can lead to a population of unfolded proteins in  
16  
17 solution prior to the formation of gaseous ions. Results from basic solutions in which the native  
18  
19 form of the protein is destabilized indicate that the majority of protein ions originating from the  
20  
21 larger droplets are formed inside of the mass spectrometer. These results are consistent with the  
22  
23 charged residue mechanism for ion formation in native mass spectrometry. Our results also  
24  
25 indicate that the assumption that ions are formed at the entrance of the mass spectrometer in  
26  
27 kinetic experiments aimed at measuring rates of chemical reactions will lead to errors.  
28  
29  
30  
31  
32

33 A larger temperature effect is observed from larger droplets formed from ammonium  
34  
35 bicarbonate compared to ammonium acetate solutions. Results from temperature melt studies  
36  
37 show that the native form of  $\beta$ -lactoglobulin is thermally less stable in ammonium bicarbonate  
38  
39 buffer. Electrothermal supercharging is also more effective in ammonium bicarbonate than  
40  
41 ammonium acetate, consistent with the proposed mechanism of the voltage induced droplet  
42  
43 heating that occurs before droplets enter the mass spectrometer.  
44  
45  
46

47 These studies demonstrate the advantages of preparing droplets with known lifetimes.  
48  
49 The use of small tips to produce droplets with short lifetimes has the advantage that the mass  
50  
51 spectra obtained under native conditions do not depend on the desolvation temperature used in  
52  
53 the mass spectrometer because ions originating from these droplets are formed outside of the  
54  
55  
56  
57  
58  
59  
60

1  
2  
3 mass spectrometer. These small tips have the additional advantage that effects of protein  
4 dimerization or aggregation that can occur in larger droplets are eliminated when the droplets  
5 contain on average much fewer than one protein molecule per droplet. Thus, in addition to the  
6 protein desalting effects reported earlier for submicron emitter tips,<sup>34,36–38</sup> these small tips should  
7 be advantageous for native mass spectrometry by eliminating artifacts of protein aggregation that  
8 can occur in droplets and any adverse effects of thermal activation in the ion source.  
9  
10  
11  
12  
13  
14  
15  
16  
17  
18

### 19 **Acknowledgments**

20  
21 This material is based upon work supported by the National Science Foundation Division of  
22 Chemistry under grant number CHE-1609866. The authors also thank Dr. Moitrayee  
23  
24  
25  
26  
27  
28  
29  
30  
31  
32  
33  
34  
35  
36  
37  
38  
39  
40  
41  
42  
43  
44  
45  
46  
47  
48  
49  
50  
51  
52  
53  
54  
55  
56  
57  
58  
59  
60

### 31 **Reference**

- 32  
33  
34 1 L. Konermann, E. Ahadi, A. D. Rodriguez and S. Vahidi, *Anal. Chem.*, 2013, **85**, 2–9.
- 35  
36 2 P. Kebarle and U. H. Verkerk, *Mass Spectrom. Rev.*, 2009, **28**, 898–917.
- 37  
38 3 M. Wilm, *Mol. Cell. Proteomics*, 2011, **10**, M111.009407.
- 39  
40 4 J. V. Iribarne and B. A. Thomson, *J. Chem. Phys.*, 1976, **64**, 2287–2294.
- 41  
42 5 I. G. Loscertales and J. Fernández De La Mora, *J. Chem. Phys.*, 1995, **103**, 5041–5060.
- 43  
44 6 M. Dole, L. L. Mack, R. L. Hines, D. O. Chemistry, R. C. Mobley, L. D. Ferguson and  
45  
46  
47  
48  
49  
50  
51  
52  
53  
54  
55  
56  
57  
58  
59  
60  
M. B. Alice, *J. Chem. Phys.*, 1968, **49**, 2240–2249.
- 7 B. E. Winger, K. J. Light-Wahl, R. R. Ogorzalek Loo, H. R. Udseth and R. D. Smith, *J.*  
*Am. Soc. Mass Spectrom.*, 1993, **4**, 536–545.

- 1  
2  
3 8 H. Metwally, Q. Duez and L. Konermann, *Anal. Chem.*, 2018, **90**, 10069–10077.  
4  
5  
6 9 C. J. Hogan, J. A. Carroll, H. W. Rohrs, P. Biswas and M. L. Gross, *Anal. Chem.*, 2009,  
7  
8 **81**, 369–377.  
9  
10  
11 10 S. K. Chowdhury, V. Katta and B. T. Chait, *J. Am. Chem. Soc.*, 1990, **112**, 9012–9013.  
12  
13  
14 11 R. L. Winston and M. C. Fitzgerald, *Mass Spectrom Rev*, 1997, **16**, 165–179.  
15  
16  
17 12 I. A. Kaltashov and S. J. Eyles, *Mass Spectrom. Rev.*, 2002, **21**, 37–71.  
18  
19  
20 13 U. A. Mirza and B. T. Chait, *Int. J. Mass. Spectrom. Ion Proc.*, 1997, **162**, 173–181.  
21  
22  
23 14 H. J. Sterling, C. A. Cassou, A. C. Susa and E. R. Williams, *Anal. Chem.*, 2012, **84**,  
24  
25 3795–3801.  
26  
27  
28 15 C. A. Cassou, H. J. Sterling, A. C. Susa and E. R. Williams, *Anal. Chem.*, 2013, **85**, 138–  
29  
30 146.  
31  
32  
33 16 X. D. Chillier, A. Monnier, H. Bill, F. O. Gülacar, A. Buchs, S. A. McLuckey and G. J.  
34  
35 Van Berkel, *Rapid Commun. Mass Spectrom.*, 1996, **10**, 299–304.  
36  
37  
38 17 K. Chingin, V. Frankevich, R. M. Balabin, K. Barylyuk, H. Chen, R. Wang and R.  
39  
40 Zenobi, *Angew. Chemie - Int. Ed.*, 2010, **49**, 2358–2361.  
41  
42  
43 18 R. M. Bain, C. J. Pulliam and R. G. Cooks, *Chem. Sci.*, 2015, **6**, 397–401.  
44  
45  
46 19 J. K. Lee, S. Kim, H. G. Nam and R. N. Zare, *Proc. Natl. Acad. Sci.*, 2015, **112**,  
47  
48 201503689.  
49  
50  
51 20 L. P. Mark, M. C. Gill, M. Mahut and P. J. Derrick, *Eur. J. Mass Spectrom.*, 2012, **18**,  
52  
53 439–446.  
54  
55  
56 21 C. M. Fisher, A. Kharlamova and S. A. McLuckey, *Anal. Chem.*, 2014, **86**, 4581–4588.  
57  
58  
59  
60

- 1  
2  
3 22 D. N. Mortensen and E. R. Williams, *Anal. Chem.*, 2015, **87**, 1281–1287.  
4  
5  
6 23 D. N. Mortensen and E. R. Williams, *J. Am. Chem. Soc.*, 2016, **138**, 3453–3460.  
7  
8  
9 24 D. N. Mortensen and E. R. Williams, *Chem. Commun.*, 2016, **52**, 12218–12221.  
10  
11 25 M. Girod, E. Moyano, D. I. Campbell and R. G. Cooks, *Chem. Sci.*, 2011, **2**, 501.  
12  
13  
14 26 E. T. Jansson, Y.-H. Lai, J. G. Santiago and R. N. Zare, *J. Am. Chem. Soc.*, 2017, **139**,  
15  
16 6851–6854.  
17  
18  
19 27 S. Zhou, B. S. Prebyl and K. D. Cook, *Anal. Chem.*, 2002, **74**, 4885–4888.  
20  
21  
22 28 M. C. C. Shastry, S. D. Luck and H. Roder, *Biophys. J.*, 1998, **74**, 2714–2721.  
23  
24  
25 29 D. N. Mortensen and E. R. Williams, *Anal. Chem.*, 2014, **86**, 9315–9321.  
26  
27  
28 30 X. Ding, Y. Yang, S. Zhao, Y. Li and Z. Wang, *Dairy Sci. Technol.*, 2011, **91**, 213–225.  
29  
30  
31 31 C. Bhattacharjee and K. P. Das, *Eur. J. Biochem.*, 2000, **267**, 3957–3964.  
32  
33  
34 32 S. G. Anema and A. B. McKenna, *J. Agric. Food Chem.*, 1996, **44**, 422–428.  
35  
36  
37 33 N. K. Kella and J. E. Kinsella, *Biochem. J.*, 1988, **255**, 113–8.  
38  
39  
40 34 Z. Xia and E. R. Williams, *J. Am. Soc. Mass Spectrom.*, 2018, **29**, 194–202.  
41  
42  
43 35 D. N. Mortensen and E. R. Williams, *Anal. Chem.*, 2016, **88**, 9662–9668.  
44  
45  
46 36 A. C. Susa, Z. Xia and E. R. Williams, *Anal. Chem.*, 2017, **89**, 3116–3122.  
47  
48  
49 37 A. C. Susa, Z. Xia and E. R. Williams, *Angew. Chemie Int. Ed.*, 2017, 1–5.  
50  
51  
52 38 A. C. Susa, J. L. Lippens, Z. Xia, J. A. Loo, I. D. G. Campuzano and E. R. Williams, *J.*  
53  
54 *Am. Soc. Mass Spectrom.*, 2018, **29**, 203–206.  
55  
56  
57 39 A. Schmidt, M. Karas and T. Dülcks, *J. Am. Soc. Mass Spectrom.*, 2003, **14**, 492–500.  
58  
59  
60

- 1  
2  
3 40 K. L. Davidson, D. R. Oberreit, C. J. Hogan and M. F. Bush, *Int. J. Mass Spectrom.*,  
4  
5  
6 2017, **420**, 35–42.  
7  
8  
9 41 L. Konermann, *J. Am. Soc. Mass Spectrom.*, 2017, **28**, 1827–1835.  
10  
11 42 E. J. Cohn and J. T. Edsall, *Proteins, Amino Acids and Peptides as Ions and Dipolar*  
12  
13 *ions*, Reinhold Publishing, New York, 1943.  
14  
15  
16 43 J. A. Gally and G. M. Edelman, *Biochim. Biophys. Acta*, 1962, **60**, 499–509.  
17  
18  
19 44 M. Gottschalk, H. Nilsson, H. Roos and B. Halle, *Protein Sci.*, 2009, **12**, 2404–2411.  
20  
21  
22 45 T. J. El-Baba, D. W. Woodall, S. A. Raab, D. R. Fuller, A. Laganowsky, D. H. Russell  
23  
24 and D. E. Clemmer, *J. Am. Chem. Soc.*, 2017, **139**, 6306–6309.  
25  
26  
27 46 J. Leonil, D. Molle, J. Fauquant, J. L. Maubois, R. J. Pearce and S. Bouhallab, *J. Dairy*  
28  
29 *Sci.*, 1997, **80**, 2270–2281.  
30  
31  
32  
33  
34  
35  
36  
37  
38  
39  
40  
41  
42  
43  
44  
45  
46  
47  
48  
49  
50  
51  
52  
53  
54  
55  
56  
57  
58  
59  
60

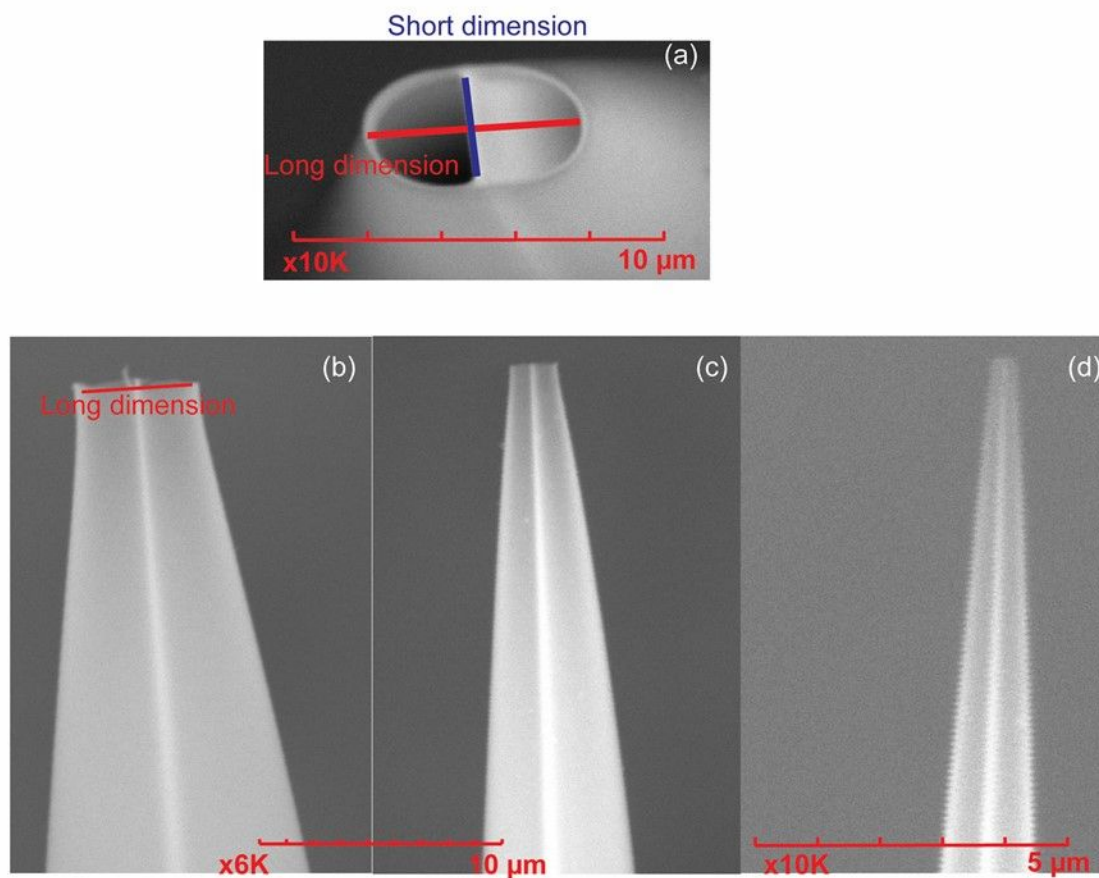


Figure 1: Scanning electron microscope images of theta emitters with different tip sizes (a) the end of an emitter tip showing the two channels with both the long (red) and short (blue) dimension labeled, (b) the long dimension side of a theta emitter tip that is 4.4 μm, (c) 1.7 μm, and (d) 317 nm. The short dimension of the emitters in (b), (c) and (d) are 2.1 μm, 1.1 μm, and 221 nm, respectively.

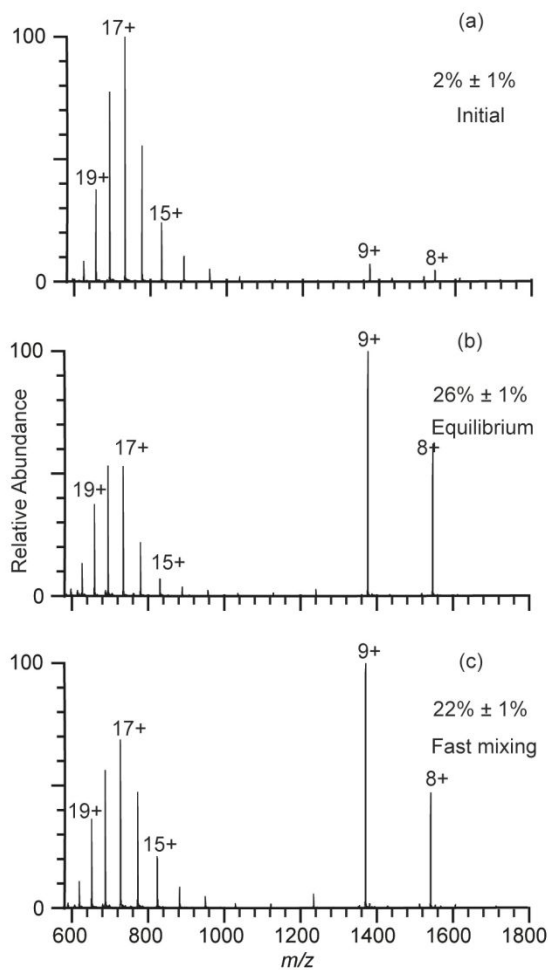


Figure 2: Electrospray ionization mass spectra for cytochrome *c* refolding experiments with a 4.4  $\mu\text{m}$  theta emitter with 10 psi backing pressure used to deduce droplet lifetime: spectra obtained for solutions consisting of (a) water with 1% acetic acid (pH = 2.8), (b) 1:1 mixture of water with 1% acetic acid and pure water at equilibrium (pH = 3.0), and (c) rapid mixing of the acidified aqueous solution used in (a) and water using a theta emitter. Percentages of folded cytochrome *c* are labeled in the spectra.

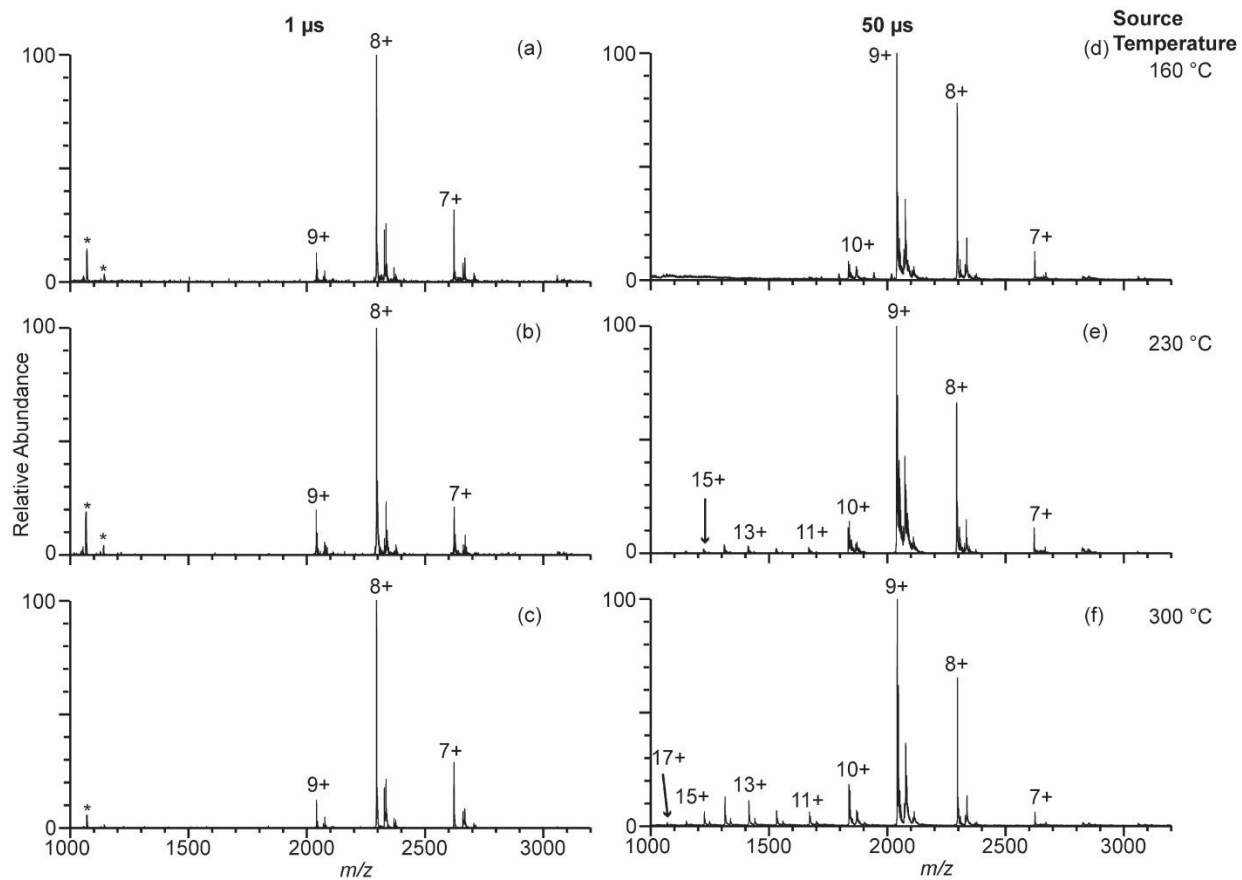


Figure 3: Electrospray ionization mass spectra obtained from solutions consisting of 10  $\mu\text{M}$   $\beta$ -lactoglobulin in 100 mM ABC using 317 nm (a-c) and 4.4  $\mu\text{m}$  (d-f) theta emitters at source temperatures of 160  $^{\circ}\text{C}$  (a, d), 230  $^{\circ}\text{C}$  (b, e), and 300  $^{\circ}\text{C}$  (c, f). The lifetime of the droplets formed from 317 nm and 4.4  $\mu\text{m}$  theta emitter is approximately 1  $\mu\text{s}$  and 50  $\mu\text{s}$ , respectively. Peaks at slightly higher  $m/z$  corresponds to lactosyl covalently bound to  $\beta$ -lactoglobulin.<sup>46</sup> \* indicates polydimethylsiloxane clusters that are present as an impurity.

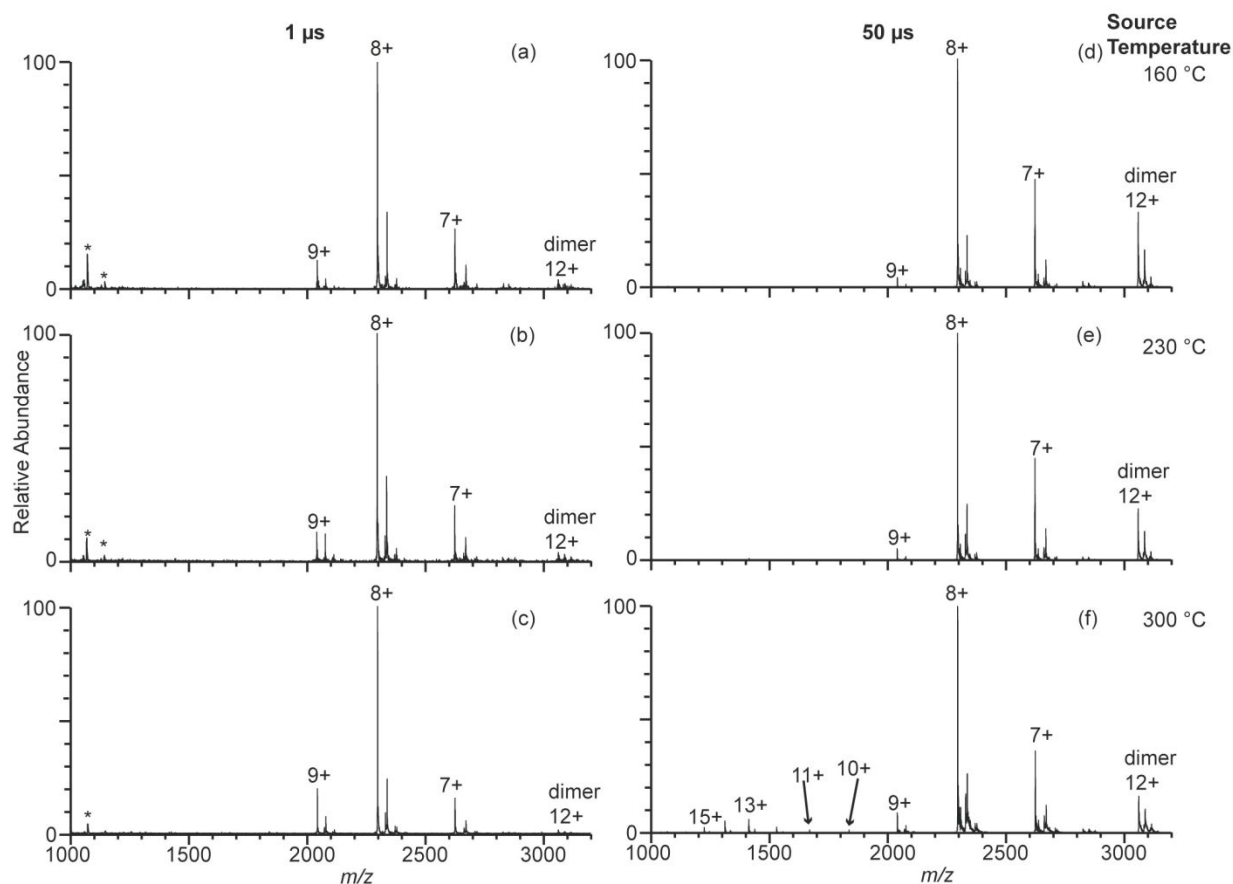


Figure 4: Electro spray ionization mass spectra obtained from solutions consisting of 10  $\mu\text{M}$   $\beta$ -lactoglobulin in 100 mM AA using 317 nm (a-c) and 4.4  $\mu\text{m}$  (d-f) theta emitters at source temperature 160  $^{\circ}\text{C}$  (a, d), 230  $^{\circ}\text{C}$  (b, e), and 300  $^{\circ}\text{C}$  (c, f). The lifetime of the droplets formed from 317 nm and 4.4  $\mu\text{m}$  theta emitter is approximately 1  $\mu\text{s}$  and 50  $\mu\text{s}$ , respectively. Peaks at slightly higher  $m/z$  corresponds to lactosyl covalently bound to  $\beta$ -lactoglobulin.<sup>46</sup> \* indicates polydimethylsiloxane clusters that are present as an impurity.

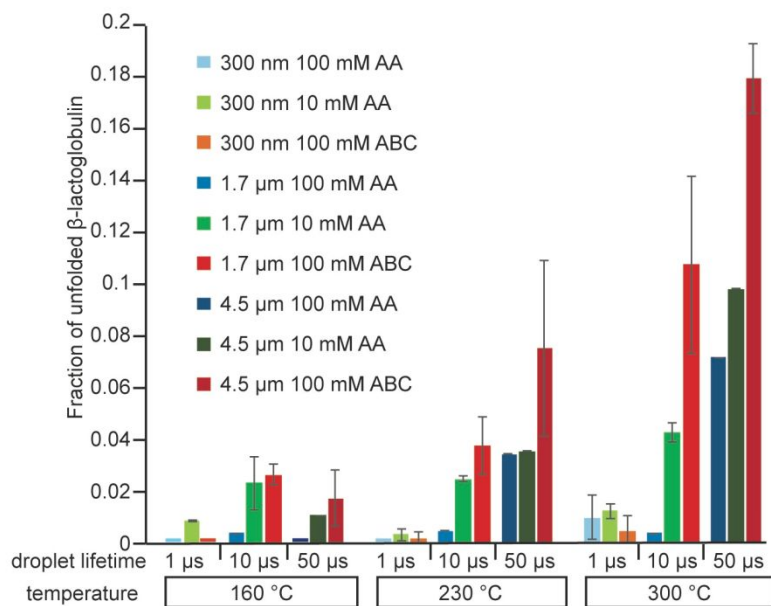


Figure 5: The fraction of unfolded  $\beta$ -lactoglobulin ions obtained from electrospray ionization using 317 nm (light shades), 1.7  $\mu$ m (medium shades), and 4.4  $\mu$ m (dark shades) theta emitters from solutions consisting of 10 mM AA (green), 100 mM AA (blue), and 100 mM ABC (red) at three different instrument source temperatures.

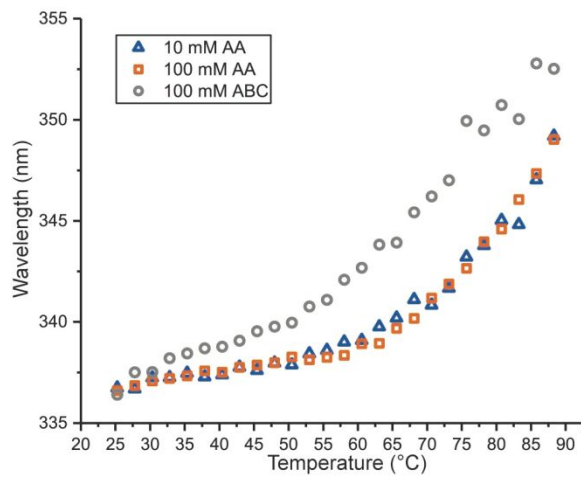


Figure 6: Temperature melt of  $\beta$ -lactoglobulin obtained by measuring the shift in the wavelength of the maximum fluorescence emission intensity of tryptophan in solutions consisting of 10 mM AA, 100 mM AA and 100 mM ABC at temperatures between 25 °C and 87.5 °C measured in 2.5 °C increments.

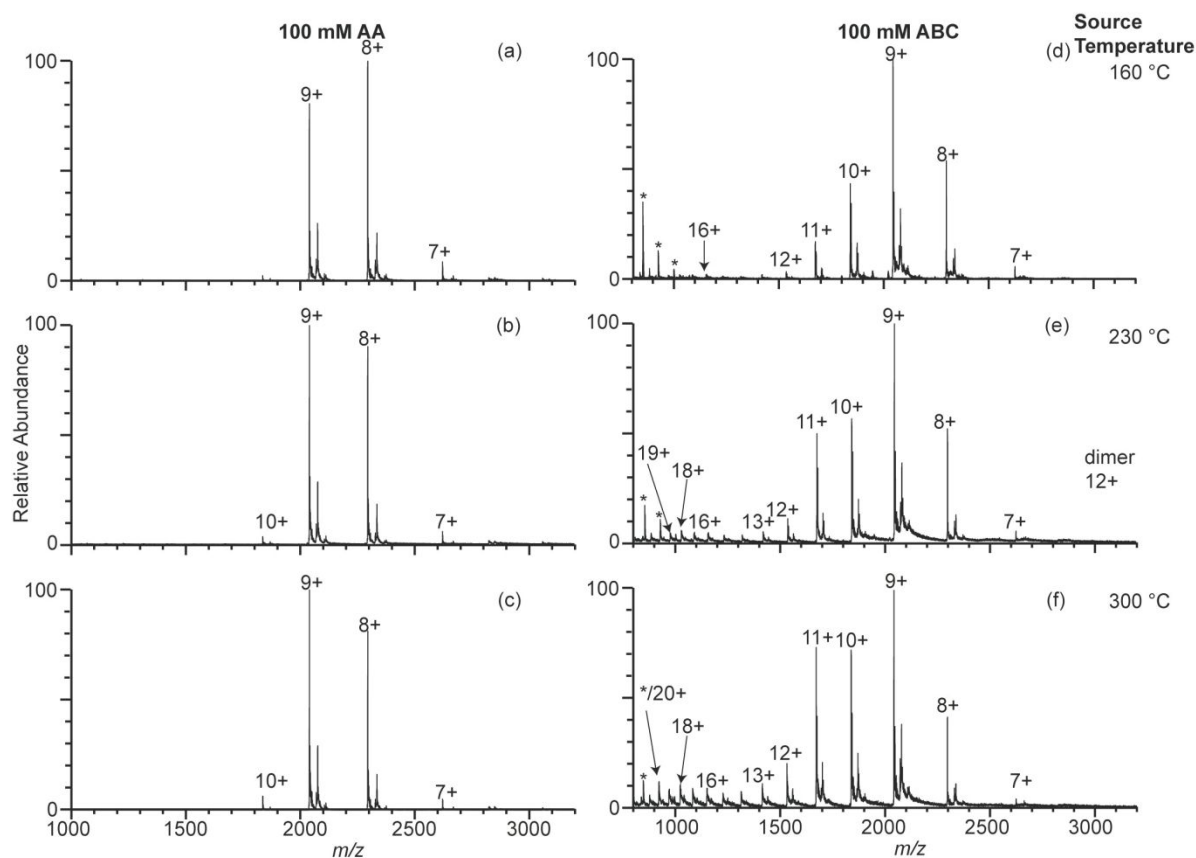
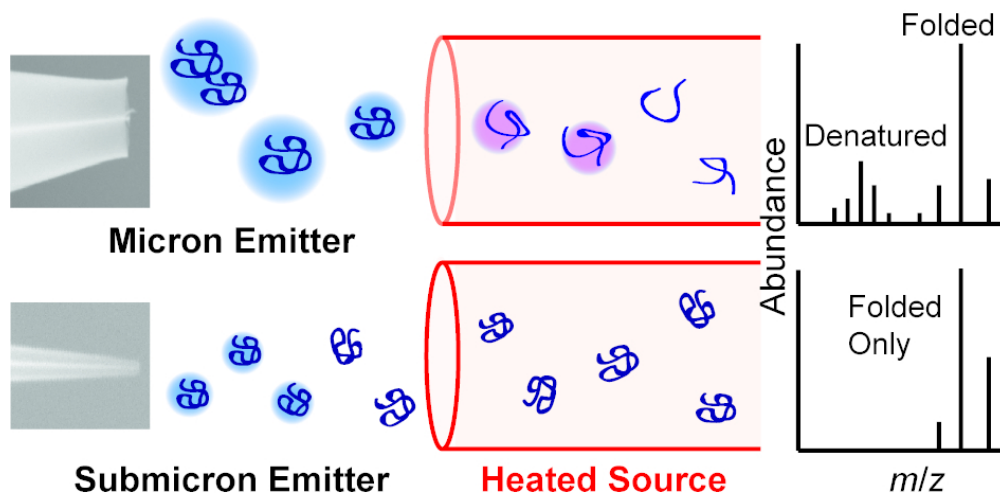


Figure 7: Electro spray ionization mass spectra obtained with electrothermal supercharging of 10  $\mu$ M  $\beta$ -lactoglobulin in 100 mM ABC and 100 mM AA at a spray voltage of 1.3 kV using 1.7  $\mu$ m single barrel emitters at source temperature 160 °C (a, d), 230 °C (b, e), and 300 °C (c, f). Peaks at slightly higher  $m/z$  corresponds to lactosyl covalently bound to  $\beta$ -lactoglobulin.<sup>46</sup> \* indicates polydimethylsiloxane clusters that are present as an impurity.



80x42mm (300 x 300 DPI)

1  
2  
3  
4  
5  
6  
7  
8  
9  
10  
11  
12  
13  
14  
15  
16  
17  
18  
19  
20  
21  
22  
23  
24  
25  
26  
27  
28  
29  
30  
31  
32  
33  
34  
35  
36  
37  
38  
39  
40  
41  
42  
43  
44  
45  
46  
47  
48  
49  
50  
51  
52  
53  
54  
55  
56  
57  
58  
59  
60